Effect of temperature and morphology on the electrical properties of PET/conductive nanofillers composites

Giuliana Gorrasi*[1], Valeria Bugatti[1], Candida Milone[2], Emanuela Mastronardo[2], Elpida Piperopoulos[2], Laura Iemmo[3] and Antonio Di Bartolomeo[3]

[1]*Department of Industrial Engineering, University of Salerno, via Giovanni Paolo II, 132 Fisciano (Salerno)-Italy-*
[2]*Department of Engineering, University of Messina, Contrada Di Dio, 1 Vill. S. Agata, Messina-Italy-*
[3]*Department of Physics "E.R. Caianiello", University of Salerno, via Giovanni Paolo II, 132 Fisciano (Salerno)-Italy-*

**e-mail: ggorrasi@unisa.it*

Abstract

Poly(ethylene terephthalate) (PET) composites were loaded with four different carbon-based fillers: functionalized carbon nanotubes (CNT), exfoliated graphite (EG), and hybrid materials such as $Mg(OH)_2$, which is primarily used as a flame retardant additive in plastics, dispersed over functionalized CNT and EG. The technology used to mix the different phases was high energy ball milling in dry conditions and at ambient temperature. Morphological organization, thermal and electrical properties of composites were evaluated and correlated with the type of filler. The electrical properties were analyzed over a wide temperature range, from 25°C to 150 °C, and correlated to the starting structural organization of the composites and the morphological transformations occurred during the thermal heating.

Keywords: PET, carbon nanotubes, exfoliated graphite, conductive composites

1. Introduction

Basic and applied research has been devoting much attention, over the past two decades, to conductive carbon based polymeric composites. The insulating properties of commodity polymers exclude them from important applications that require moderate or high electrical conductivity. It has been widely demonstrated that carbon based fillers (carbon nanotubes, carbon nanofibers graphites and exfoliated graphites, graphenes, etc…) lead to remarkable increase in the electrical conductivity of the composites near the percolation threshold [1-5]. This is due to a continuous conductive network formed in particular arrangements by the

conductive carbon fillers within the polymer matrices. Low percolation threshold is highly desirable. It ensures lightweight, low cost, high mechanical strength and facile processing of the composites. Furthermore, it is well known that thermoplastic polymers undergo thermal transitions at given temperatures; such transitions can occur in the material during the usual utilization conditions, and can strongly influence their morphological organization, and the resulting physical properties. Poly(ethylene terephthalate) (PET) is an engineering thermoplastic polymer that covers a wide field of applications, like packaging and fiber production. It has been widely processed in blends, composites and nano-composites to improve its physical properties and impart novel functionalities [6-9]. In the next years, PET consumptions is expected to significantly increase over the traditional materials (glass, metals, ceramics, paper), and the fluctuations of oil price, associated to a greater consumer awareness of sustainability issues, has originated a growing demand for a new generation of engineering bio-plastics. The non-petroleum derived PET is one of the most promising new bio-plastic. Bio-PET, also called "bio-sourced PET", is a polyethylene terephthalate resin manufactured from the same petroleum sourced element terephthalic acid, but from bio-sourced ethylene glycol. A fundamental goal for the industry is to replace this terephthalic acid with a bio-based version, so recent evolutions in this field point towards a fully bio-sourced PET production in the next future. Differently from many others engineering polymers, there are only few studies related to PET nanocomposites. This is mainly due to the difficulty to produce PET nanocomposites by melt compounding, for the thermal degradation of polymer chains inducted by high temperatures and shear stresses [10]. An efficient alternative to melt mixing, or solvent casting, has been proved to be High Energy Ball Milling (HEBM) at ambient temperature [11, 12]. Intimate mixing in the solid state, between two or more species, is promoted by mechanical energy, rather than by solvents or high temperatures. The subject of this work is the preparation of novel PET composites, through HEBM, loaded with four different carbon-based fillers: exfoliated graphite (EG), functionalized carbon nanotubes (CNT), and hybrid materials as $Mg(OH)_2$, which is primarily used as a flame retardant additive in plastics, dispersed over EG and functionalized CNT. Morphology, thermal and electrical properties of composites' systems were evaluated and correlated with the filler composition. The electrical properties were investigated over a wide temperature range (25°C ÷150 °C). The electrical response was correlated to the starting structural organization of the composites and the morphological transformations that occur during the thermal heating.

2. Experimental

2.1 Materials

PET, supplied by M&G Polimeri Italia S.p.A, is commercially named CLEARTUF P76 (intrinsic viscosity is 0.74 dL/g).

EG supplied by TIMCAL Ltd is commercially named TIMREX C-THERM 002.

Carbon Nanotubes, prepared accordingly with procedure reported elsewhere [13] were funzionalized by oxidation in nitric acid vapour (HNO_3) at T = 135 °C for 120 min, following the procedure reported in ref. [14].

Hybrids fillers consisting of ($Mg(OH)_2$ dispersed over EG and functionalized CNTs were prepared by deposition-precipitation of magnesium hydroxide over carbonaceous supports, according with the procedure reported elsewhere [15]. The amount of $Mg(OH)_2$ in the hybrid is ~ 50 wt.%

2.2 Incorporation of carbon based fillers into PET

The incorporation of the fillers into PET was achieved by the HEBM method. Powders composed of PET and the fillers, after vacuum drying 24 h, were milled at room temperature in a Retsch (Haan, Germany) Planetary Ball Mill (model PM100). The weight percent of filler was 3% in the case of EG and CNT and 6% in the case of $Mg(OH)_2$/EG and $Mg(OH)_2$/CNT in order to kept constant at 3 wt.% the carbon phase composition for all preparations. The powders were milled in a cylindrical steel jar of 12 cm^3 with three steel balls of 10 mm of diameter. The rotation speed was 450 rpm, with a milling time of 1 hour. The pure PET, taken as reference, was milled in the same experimental conditions as the composites.

2.3 Film preparation

The milled powders were molded in a Carver laboratory press between two Teflon sheets, at 270 °C, followed by rapid cooling at natural convection. Films about 300 μm thick were obtained and analyzed. Samples codes and composition are listed in Table 1.

2.3 Methods of investigation

Scanning Electron Microscopy (SEM) analysis were performed by means of a JSM-5600LV instrument operating at 20 kV.

X-ray powder diffraction measurements (XRD) were performed with a Brucker diffractometer (equipped with a continuous scan attachment and a proportional counter) with Ni-filtered Cu Kα radiation (λ=1.54050 Å).

Differential scanning calorimetry (DSC) were carried out using by means of a DTA Mettler Toledo (DSC 30) under nitrogen atmosphere. The films were submitted to the following thermal cycle: 25°C ÷ 300°C at a heating rate of 20 °C/min.

Attenuated total reflection (ATR) infrared spectra were recorded by a Bruker spectrometer, model Vertex 70. The incidence angle of the radiation on the ATR crystals was 45°. Analyses were performed by acquiring the background in air and accumulating 32 spectra for each measurement at a resolution of 4 cm^{-1}.

Thermogravimetric analyses (TGA) were carried out under air flow with a Mettler TC-10 thermobalance from room temperature to 1000 °C with a heating rate of 10 °C/min.

Electrical measurements were performed in a Janis ST-500 temperature-controlled probe station, connected to a Keithley 4200-SCS semiconductor parameter analyzer, equipped with high-power source-meter units (current up 0.1 A at 210 V). A two probe configuration, where we forced a voltage and measured a current, was used for the conductivity measurements at given temperatures in the 25-150 °C range and at an air pressure of 30 mbar to prevent moisture formation or dust deposition.

3. Results and discussion

We first discuss the morphology of carbon based fillers as inferred by SEM analysis. EG consists of numerous and extremely thin sheets with irregular shape (Figure 1 a), while CNTs appear as highly entangled tubes (Figure 1 b) with several graphitic planes forming their walls (inset of Figure 1 b). XRD analysis in a 2-theta range between 10° and 80° (not shown for the sake of brevity) evidences in both samples peaks relative to the graphite phase (2θ: 26.5°, 42.5°, 45°, 51°, 55°, 78°) in agreement with the standard data JCPDS 25-0284. XRD spectra of hybrids materials, prepared upon precipitation of $Mg(OH)_2$ over EG or CNT, show typical reflection of graphite together with reflections arising from hexagonal brucite phase (Figure 2). The lower intensity of the reflection peaks of graphite in CNT can be ascribed to the lower crystallinity and/or to size effect.

In the case of $Mg(OH)_2$/EG hybrid, EG flakes are not visible anymore and large aggregates mainly exposing smaller brucite platelets are evidenced (Figure 1 c). The attribution of external platelets to brucite is confirmed by the comparison with the morphology of sole precipitated $Mg(OH)_2$ (inset of Figure 1 c). Accordingly, it can be concluded that EG is covered and encapsulated by the hydroxide phase. A densely packed structure is formed upon precipitation of $Mg(OH)_2$ over CNT: in this case an external $Mg(OH)_2$ coat are visible (white arrow) together with a more intimate mixing between the two phases, carbon nanotubes and $Mg(OH)_2$ (black arrow).

Figure 3 reports the XRD spectra of the PET films loaded with the different fillers. It is interesting to note that the addition of EG and CNTs to PET does not modify the amorphous arrangement of the macromolecular chains observed in un-loaded PET (Figure 3 a). It is noteworthy that the graphitic structure of the filler is maintained upon HBEM, as inferred by the presence of the reflection at $2\theta = 26.5°$ related to the most intense peak due to (002) plane of graphite. The lower intensity of the (002) reflection peak in the PET_CNT sample reflects the lower intensity observed in the starting material. As a main difference, the addition of $Mg(OH)_2$/EG and $Mg(OH)_2$/CNT fillers promotes the PET crystallization, as demonstrated by the typical reflection peaks of crystalline PET at $2\theta = 16.3°, 17.6°, 18.8°, 21.6°, 22.8°, 26.1°$ (Figure 3 b). Furthermore, reflection of graphitic (002) plane is better visible in the sample PET_M_EG while in the case of PET_M_CNT the absence of a definite peak could be due to the lower intensity previously observed.

The DSC thermograms, reported in Figure 4, confirm the structural organization of the samples, evidenced from XRD. The thermogram of pure PET is typical of amorphous PET sample. The Tg is located at 77°C, the cold crystallization peak is centered at about 140°C, and the fusion of crystalline phase formed during the heating scan occurs at about 250°C. Similar trends hold for samples filled with EG and CNTs, for which the crystallization exotherms are located at temperature lower than 140°C (i.e. about 127°C) for the nucleating effect of the fillers. As expected for the starting amorphous structures, the calculated crystallinity degree, evaluated subtracting the heat of cold crystallization from the heat of melting, and dividing for the enthalpy of the theoretical heat of melting for 100% crystalline PET (ΔH_0=105.97 J/g) [16], we found a value around 1.5-2.0%. For samples filled with $Mg(OH)_2$/EG and $Mg(OH)_2$/CNTs, in agreement with XRD spectra, we observe a degree of crystallinity of 18% and 27%, respectively.

ATR spectra were collected on all samples in order to evaluate the evolution of conformational order of macromolecular PET chains. PET in the crystalline phase assumes a full trans conformation, but it is mostly in gauche conformation in the amorphous phase [17]. The two conformers have several distinct IR absorptions bands that make it possible to follow the conformational changes, as well as the crystallization process, by infrared spectroscopy [18, 19]. The wagging bands of the glycol segment in the trans conformation at 1340 cm^{-1}, was conveniently selected in this work for quantitative purpose. Furthermore, the band at 1410 cm^{-1}, typically used as reference band [20], lies in similar position and its use for normalization purpose is thus acceptable [21], enabling a quantitative comparison. From the ATR spectra, we obtained the ratio between the band sensitive to the trans conformation of glycolic groups (1340 cm^{-1}) and the reference band (1410 cm^{-1}) for all samples. Data are reported in Table 2. As expected for growing crystallinity, we observe an increase of trans conformers, with the maximum ratio for sample PET_M_CNT, that shows the higher crystallinity.

The thermal degradation behaviour was evaluated on PET and composites with different fillers in air atmosphere, and is shown in Figure 5. Differential Thermogravimetric curves show that the degradation of PET and its composites happens in two steps. The main decomposition step, due to the oxidative degradation of the starting materials, occurs in the temperature range 350°C-450 °C reaching the maximum rate at Tp= 419 °C while the second one, attributed to the consumption of char under the air atmosphere [22, 23] occurs in the temperature range 470°C-550°C reaching the maximum rate at Tp= 429 °C. As common feature, it is observed that upon addition of fillers, regardless the typology, the first decomposition step shifts to higher temperature. The maximum-rate degradation temperature (Tp) varies between 437°C-442 °C, that is from 10 to 12 °C higher than in unfilled PET. This effect is mainly caused by the carbonaceous filler, while $Mg(OH)_2$ seems not to play any role. In fact Tp doesn't change in the presence or the absence of hydroxide. In the presence of $Mg(OH)_2$ (PET_M_EG and PET_M_CNT samples) a small shoulder appears at lower temperature (377 °C) due to the dehydration of hydroxide to MgO and the consequent loss of water. The high temperature peak, i.e. char oxidation, seems to be less influenced by the presence of filler. Mass loss occurs in the same range of temperature observed for the unfilled PET and the total area is almost constant for all the samples investigated but PET_EG where a slight decrease is observed. On the basis of the above results, it can be concluded that the addition of carbonaceous filler, regardless the typology, enhances the thermal stability of polyester chains due to a barrier effect of the nano-filler dispersed into the PET matrix, respect the air gases permeating through the composites and likely also to the volatile decomposition products. We cannot ruled out that carbonaceous

198 filler acts as a trap towards the polymer peroxyl radical formed during the thermo-oxidative
199 decomposition, thus preventing their recombination [24-26].
200 Electrical performances of the different PET composites were measured over a variable voltage
201 range (typically < 15 V), chosen to keep the current below 10 mA and prevent possible Joule
202 heating induced-damage. The voltage bias was applied across the thickness of the sample (~150
203 μm), thus producing a maximum electric field of $\sim 10^5\ V/m$. The current-voltage (I-V)
204 characteristics showed linear behaviour (an example is displayed in Figure 6 for PET_EG
205 sample) and their slope was used to evaluate the conductance $G = I/V$ (S). The electrical
206 conductivity σ(S/m) was then extracted from the measured contact area A and sample thickness
207 t, as $\sigma = Gt/A$. Being the CNTs or the EG the conducting nanoparticles, the current flow is
208 attributed to their load and degree of dispersion. Figure 7 shows σ as a function of temperature
209 for the four samples under study. The PET matrix has an insulating behaviour with an electrical
210 conductivity around $3 \cdot 10^{-17}$ S/m, that is below the sensitivity limit of our measurement setup on
211 the whole investigated temperature range [22]. An insulating behaviour is shown by PET_EG
212 and PET_CNT samples at ambient temperature, with electrical conductivity two (PET_EG) or
213 three (PET_CNT) orders of magnitude higher than the PET matrix, implying that the 3%wt
214 concentration of filler is not enough to achieve the percolation threshold. The electrical
215 behaviour of these two samples, as function of temperature, calls for a particular attention. The
216 conductivity increases slowly up to the glass transition temperature of the composites (i.e. ~
217 77°C), and then increases much faster up to 150°C, that is the crystallization temperature of the
218 samples (see DSC analysis in Figure 4). The raising temperature activates the motion (hopping)
219 of electrons from one isolated state to the next. The result is an ohmic conduction process, with
220 characteristic exponentially dependent on temperature. The ohmic process is the dominant
221 electrical conduction mechanism in insulators at low bias and high temperature [27], and its
222 voltage and temperature dependence is described by the equation:

223 $$I = G_0 V \ \exp\left(-\frac{E_{ac}}{kT}\right) \qquad (1)$$

224 Where $G = G_0 \exp\left(-\frac{E_{ac}}{kT}\right)$ is the conductance at temperature T, k is the Boltzmann constant
225 and E_{ac} the electron activation energy. G_0 is the value of the conductance when the electron
226 average hopping barrier vanishes. We can turn the expression for *G*, or the equivalent one for
227 the conductivity $\sigma = Gt/A$, into a straight-line plot by taking the logarithm of both sides:

228 $$\log \sigma = \log \sigma_0 - \log_{10} e \cdot \frac{E_{ac}}{kT} \qquad (2)$$

The ohmic conduction model in the PET_EG and PET_CNT samples at high temperature is confirmed both by the linear I-V characteristics (Figure 6) and by the Arrhenius plot of the conductivity versus temperature ($\log \sigma \; vs. 1000/T$ plot) of Figure 8. Interestingly, the activation energy above the glass transition temperature of the PET_EG sample is 3.3 eV, which is the typical electron barrier energy of a good insulator such as SiO_2. The activation energy of 1.6 eV of PET_CNT sample is lower; however, its conductivity is lower than that of the PET_EG sample due to the smaller σ_0, as it can be verified by extrapolating the Arrhenius plot to $\frac{1}{T} \to 0$. The lower activation energy corresponds to reduced average barrier between CNTs and PET matrix, while the suppressed high temperature conductivity of the PET_CNT sample can be ascribed to less dispersion of CNTs with respect to EG in the PET matrix. Remarkably, both PET_EG and PET_CNT samples point toward an increasing conductivity with the increasing degree of crystallinity.

The electrical conductivity of samples PET_M_CNT and PET_M_EG, that appear semi-crystalline from XRD and DSC analysis, is about 15 orders of magnitude higher than that of unfilled PET, and is constant with temperature, in the whole investigated range. Experimental data and structural analysis suggest that, for the considered PET composites, the structural organization of the crystalline phase and the conductive filler is more important than the temperature of the experiment. In the amorphous samples, macromolecular chains separate the conductive fillers (i.e. CNT and EG) hindering the percolative network for the charge transport. The increasing of macromolecular mobility after the Tg and the crystallization phenomenon, either during the thermal scan or during the manufacturing of the samples, generates a crystalline phase in presence of the conductive fillers. The process of cold crystallization for samples PET_CNT and PET_EG, and crystallization from the melt most probably tend to expel the conductive fillers from the crystalline phases favouring their contact and then yielding the very high electrical conductivity. These aspects were already emphasized in high-density polyethylene (HDPE) [28], and Polystyrene (PS) filled with CNTs and submitted to thermal annealing at temperature higher than the glass temperature [29, 30]. The presence of residual stresses at the interfaces between CNTs and PS matrix, which may be removed through macromolecular relaxation induced by the thermal annealing, was suggested to enable the formation of additional ordered hexagonal structures of CNTs. The higher the residual stress, the higher the formation of additional ordered hexagonal structures, the higher the increment of the electrical conductivity after thermal annealing. In the case of HDPE, it was concluded that in semicrystalline polymers the very fine carbon based filler aggregates tend to concentrate in

amorphous regions. During the crystallization and/or annealing process a major part of the carbon filler aggregates is rejected into inter-spherulitic boundaries and the rest may be located in amorphous regions within the spherulities. As a result, the threshold percolation concentration in semicrystalline systems is lower than in amorphous polymers.

4. Concluding remarks

Morphology, thermal and electrical properties of composites such as Poly(ethylene terephthalate) loaded with CNT, EG and hybrid materials as $Mg(OH)_2$ dispersed over functionalized CNTs and EG were investigated. All composites, prepared by means of HBEM method, 3 wt% of carbonaceous conductive filler (EG or CNTs). The properties of composites were compared with those of pure PET, taken as reference, milled in the same experimental conditions. As main results it was found that the addition of EG and CNTs to PET does not modify the amorphous arrangement of the macromolecular chains observed in un-loaded PET while the addition of $Mg(OH)_2$/EG and $Mg(OH)_2$/CNT fillers promotes the PET crystallization. The addition of carbonaceous filler, regardless the typology, enhances the thermal stability of polyester chains due to a barrier effect of the nano-filler dispersed into the PET matrix.

At given temperature the electrical conductivity ranks in the order:

PET<< PET_CNT<PET_EG<< PET_M_EG<PET_M_CNT.

An increase of electrical conductivity with temperature, which fits into a thermally activated hopping model, was observed on PET_CNT and PET_EG samples. Instead, a conductivity independent of temperature was found on more conducting PET_M_CNT and PET_M_EG samples over the investigated range. These results suggest that structural organization of composites plays a major role in lowering the percolation threshold than temperature. The higher the degree of crystallinity of composite more favorite is the formation of the percolative network for the charge transport.

5. References

1) Punetha VD, Rana S, Yoo HJ, Chaurasia A, McLeskey Jr JT, Ramasamy MS, Sahoo NG, Cho JW. Functionalization of carbon nanomaterials for advanced polymer nanocomposites: A comparison study between CNT and grapheme. Progress in Polymer Science 2017; 67: 1-47

2) Mutiso RM, Winey KI. Electrical properties of polymer nanocomposites containing rod-like nanofillers Review. Progress in Polymer Science 2015; 40: 63-84

3) Radzuan NAM, Zakaria MY, Sulong AB, Sahari J. The effect of milled carbon fibre filler on electrical conductivity in highly conductive polymer composites. Composites Part B: Engineering 2017; 110: 153-160

4) Zakaria MR, Kudus MHA, Akil HMd, Thirmizir MZM. Comparative study of graphene nanoparticle and multiwall carbon nanotube filled epoxy nanocomposites based on mechanical, thermal and dielectric properties. Composites Part B: Engineering 2017; 119: 57-66

5) Guadagno L, Naddeo C, Raimondo M, Barra G, Vertuccio L, Russo S, Lafdi K, Tucci V, Spinelli G, Lamberti P. Influence of carbon nanoparticles/epoxy matrix interaction on mechanical, electrical and transport properties of structural advanced materials. Nanotechnology 2017; 28: 1-20

6) Visakh PM, Liang M. Poly (Ethylene Terephthalate) Based Blends, Composites and Nanocomposites. Elsevier 2015.

7) Ravindranath K, Mashelkar RA. Polyethylene terephthalate-II. Engineering analysis. Chemical Engineering Science 1986; 41: 2969-2987

8) Nanni F, Mayoral BL, Madau F, Montesperelli G, McNally T. Effect of MWCNT alignment on mechanical and self-monitoring properties of extruded PET-MWCNT nanocomposites. Composites Science and Technology 2012; 72: 1140-1146

9) Gorrasi G, Senatore V, Vigliotta G, Belviso S, Pucciariello R. PET–halloysite nanotubes composites for packaging application: Preparation, characterization and analysis of physical properties. European Polymer Journal 2014; 61: 145–156

10) Razzak A, Jabarin A. Processing characteristics of poly(ethylene terephthalate): hydrolytic and thermal degradation. Polymer International 2002; 51: 164-173

11) Gorrasi G, Sorrentino A. Mechanical milling as a technology to produce structural and functional bio-nanocomposites. Green Chemistry 2015; 17: 2610-2625

12) Delogu F, Gorrasi G, Sorrentino A. Fabrication of polymer nanocomposites via ball milling: Present status and future perspectives. Progress in Materials Science 2017; 86: 75-126

13) Messina G, Modafferi V, Santangelo S, Tripodi P, Donato MG, Lanza M. Large-scale production of high-quality multi-walled carbon nanotubes: role of precursor gas and of Fe-catalyst support. Diam Relat Mater 2008; 17: 1482–8

14) Milone C, Piperopoulos E, Ansari S, Faggio G, Santangelo S. Highly versatile and efficient process for CNT oxidation in vapor phase by means of $Mg(NO_3)_2$- HNO_3 - H_2O ternary mixture. Fullerene Nanotube Carbon Nanostructure 2015; 15: 1–5

15) Mastronardo E, Bonaccorsi L, Kato Y, Piperopoulos E, Lanza M, Milone C. Thermochemical performance of carbon nanotubes based hybrid materials for $MgO/H_2O/Mg(OH)_2$ chemical heat pumps. Applied Energy 2016; 181: 232–243

16) He MJ, Chen WX, Dong XX. Polymer physics, Fudan University Press, Shanghai 1991

17) Lin SB, Koenig JL. A kinetic analysis of the gauche-trans isomerization in semicrystalline poly (ethylene terephthalate). J Polym Sci: Polym Phys 1983; 21(11): 2365-78

18) Lin SB, Koenig JL. Spectroscopic characterization of the rotational conformations in the disordered phase of poly (ethylene terephthalate). J Polym Sci: Polym Phys 1982; 20(12): 2277–95

19) Cole KC, Ajji A, Pellerin É. New insights into the development of ordered structure in poly (ethylene terephthalate).1.Results from external reflection infrared spectroscopy. Macromolecules 2002; 35(3): 770–84

20) Cole KC, Ben Daly H, Sanschagrin B, Nguyen K, Ajji A. A new approach to the characterization of molecular orientation in uniaxially and biaxially oriented samples of poly (ethylene terephthalate). Polymer 1999; 40(12): 3505–13

21) Kirov KR, Assender HE. Quantitative ATR-IR analysis of anisotropic polymer films: surface structure of commercial PET. Macromolecules 2005; 38(22): 9258-65

22) Mc Crossan K, Mc Clory C, Mayoral B, Thompson D, Mc Connell D, Mc Nally T. Composites of poly(ethylene terephthalate) and multi-walled carbon nanotubes, in: T. McNally, P. Pötschke (Eds), Polymer–Carbon Nanotube Composites Preparation, Properties and Applications. Woodhead Publishing Series in Composites Science and Engineering 2011; 545–586

23) Gorrasi G, Milone C, Piperopoulos E, Pantani R. Preparation, processing and analysis of physical properties of calcium ferrite-CNTs/PET nano-composite. Composites Part B: Engineering 2015; 81: 44-52

24) Teli MD, Kale RD. Polyester Nanocomposite Fibers With Improved Flame Retardancy and Thermal Stability. Polym. Eng. Sci. 2012; 52: 1148–1154

25) Levchik SV, Weil ED. A review on thermal decomposition and combustion of thermoplastic polyesters. Polymers for Advanced Technologies 2004; 15 (12): 691-700

26) Li ML, Jeong YG. Poly(ethylene terephthalate)/exfoliated graphite nanocomposites with improved thermal stability, mechanical and electrical properties. Composites Part A-Applied Science and Manufacturing 2011; 42 (5): 560-566

27) Sze SM, Ng KK. Physics of semiconductor devices, John Wiley & Sons, Hoboken, New Jersey 2007

28) Narkis M, Vaxman A. Resistivity behavior of filled electrically conductive crosslinked polyethylene. J Appl Polym Sci 1984; 29: 1639-1652

29) Zhang W, Dehghani-Sanij AA, Blackburn RS. Carbon based conductive polymer composites. J Mater Sci 2007; 42: 3408-3418

30) Fei G, Gong Q, Li D, Lavorgna M, Xia H. Relationship between electrical conductivity and spatial arrangements of carbon nanotubes in polystyrene nanocomposites: The effect of thermal annealing and plasticization on electrical conductivity. Composites Science and Technology 2017; 146: 99-109

Table 1: Samples and composition

Sample code	Composition			
	PET (wt.%)	EG (wt.%)	CNT (wt.%)	$Mg(OH)_2$ (wt.%)
PET	100	-	-	-
PET_CNT	97	-	3	-
PET_EG	97	3	-	-
PET_M_EG*	94	3	-	3
PET_M_CNT*	94	-	3	3

*Composites prepared with hybrid $Mg(OH)_2$/EG and $Mg(OH)_2$/CNT containing 50 wt.% of $Mg(OH)_2$

Table 2: Ratio between band sensitive to the trans conformation of glycolic groups (1340 cm^{-1}) and the reference band (1410 cm^{-1}) for PET and composites

Sample	A_{1340}/A_{1410}
PET	0.23
PET_EG	0.21
PET_CNT	0.25
PET_M_EG	0.78
PET_M_CNT	1

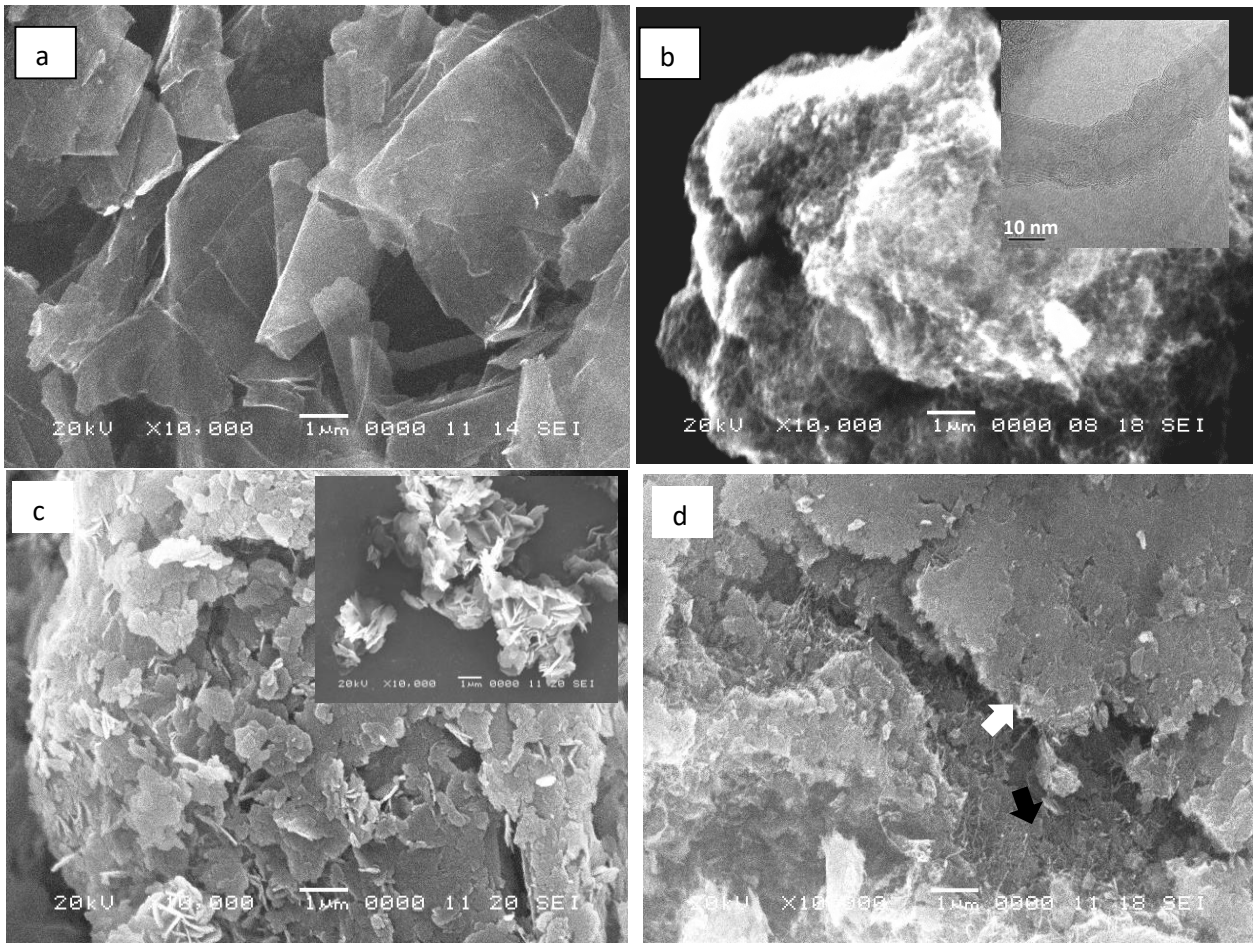

Figure 1: SEM micrograph of : EG (a), CNT(b), $Mg(OH)_2$/EG (c) and $Mg(OH)_2$/CNT (d).
Inset of figure (c) represents the morphology of sole $Mg(OH)_2$

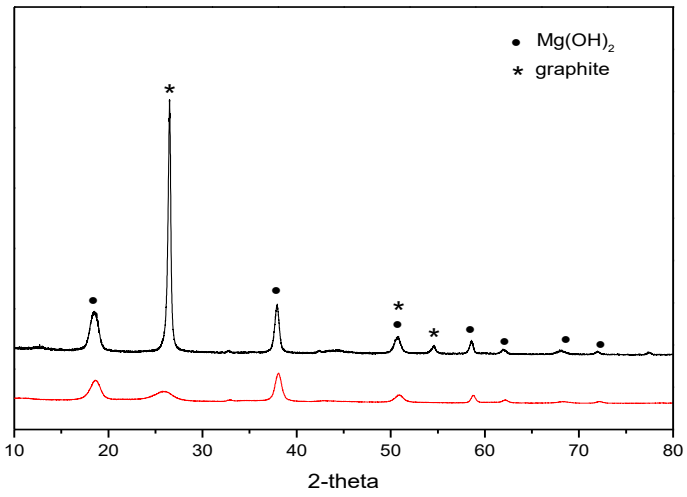

Figure 2: XRD of hybrids fillers $Mg(OH)_2$/EG (black line) and $Mg(OH)_2$/CNT (red line)

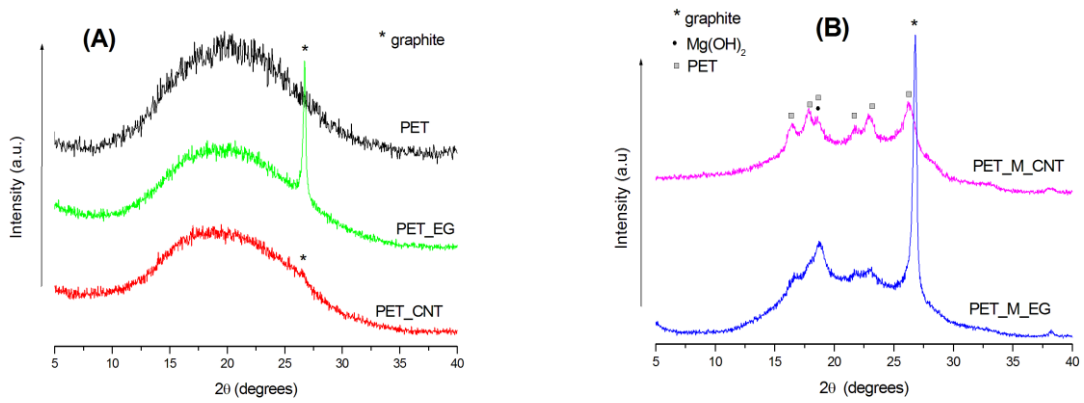

Figure 3. XRD analysis of PET and related composites

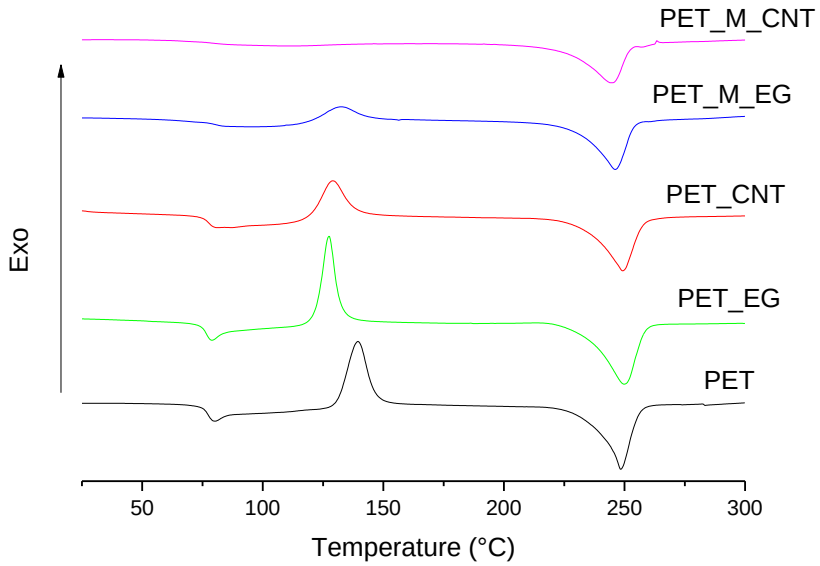

Figure 4. DSC analysis of PET and related composites

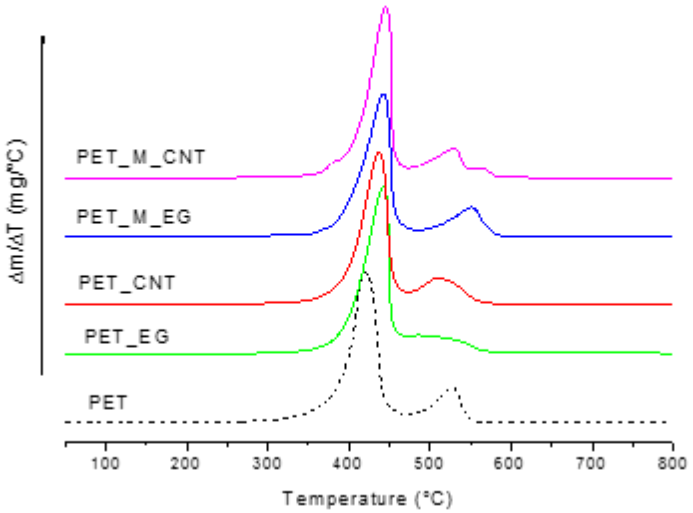

Figure 5. Differential Thermogravimetric curves, in air, of PET and related composites

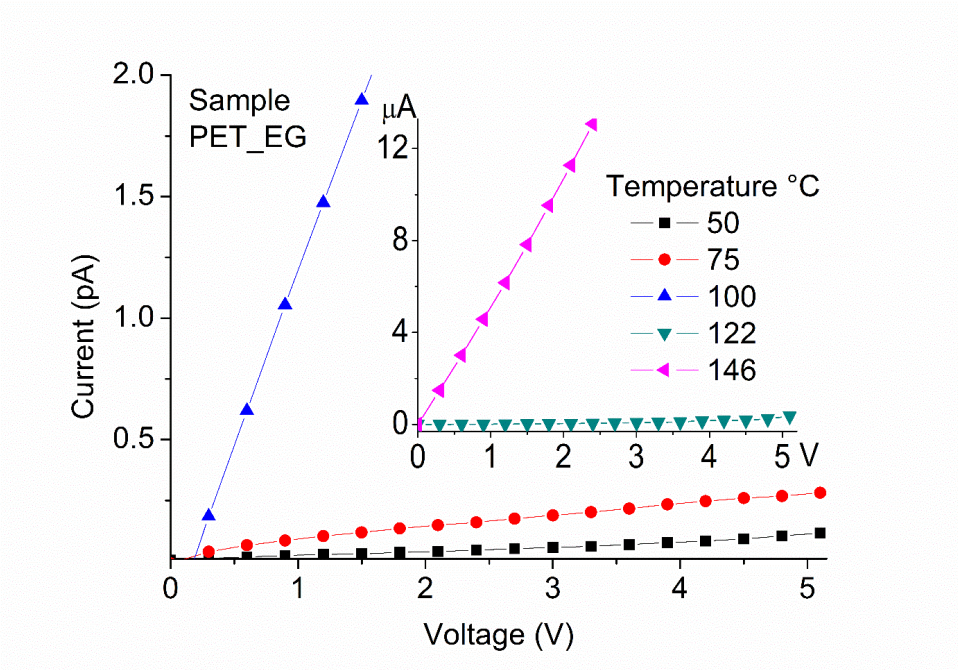

Figure 6: Current-voltage (I-V) characteristics of PET_EG sample at different temperatures.

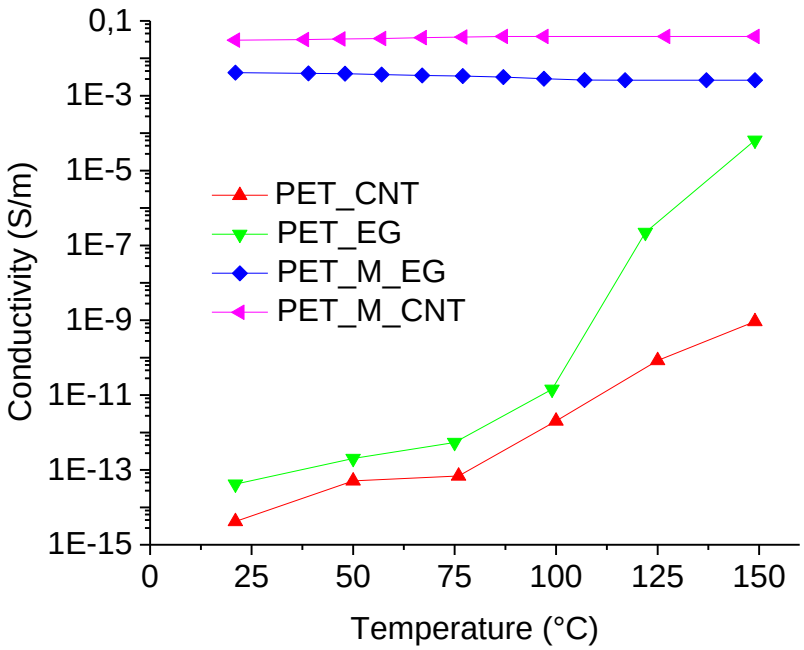

Figure 7. Electrical conductivity as function of temperature for the samples under study

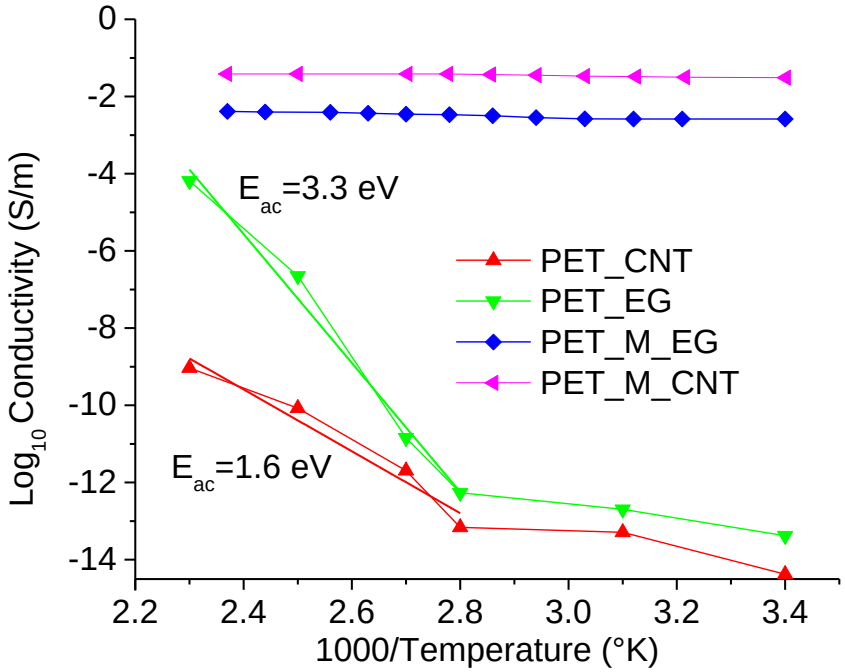

Figure 8. Arrhenius plot of the conductivity of the samples under study from which the activation energies are extracted.